

CrossMark
click for updatesCite this: *RSC Adv.*, 2016, 6, 108125

Active hydrogenation Rh nanocatalysts protected by new self-assembled supramolecular complexes of cyclodextrins and surfactants in water†

Nguyet Trang Thanh Chau,^a Stéphane Menuel,^b Sophie Colombel-Rouen,^a Miguel Guerrero,^{cd} Eric Monflier,^b Karine Philippot,^{cd} Audrey Denicourt-Nowicki^{*a} and Alain Roucoux^{*a}

The stability of inclusion complexes between randomly methylated β -cyclodextrin (RaMeCD) or its leucine-grafted analogue (RaMeCDLeu) with two hydroxylated ammonium surfactants was investigated. The binding isotherms and complexation constants were measured using the Isothermal Titration Calorimetry (ITC) technique. These host-guest inclusion complexes were used as protective agents during the formation of rhodium(0) nanoparticles by chemical reduction of rhodium trichloride in water. The amount of protective agent was adjusted in order to ensure both stability and reactivity of the rhodium nanocatalysts under the catalytic conditions. The size and dispersion of air-stable and water-soluble rhodium suspensions were determined by Transmission Electron Microscopy (TEM) analyses. These spherical nanoparticles, with sizes between 1.20 to 1.50 nm according to the nature of inclusion complexes, were evaluated in the biphasic hydrogenation of various reducible compounds (olefins, linear or aromatic ketones), showing promising results in terms of activity and selectivity.

Received 31st August 2016
Accepted 2nd November 2016

DOI: 10.1039/c6ra21851b

www.rsc.org/advances

Introduction

The development of highly selective and readily recyclable catalysts,¹ as well as the substitution of volatile organic solvents with novel reaction media (*e.g.* ionic liquids, supercritical fluids or water),^{2,3} constitute crucial parameters in the quest towards sustainable and more environmentally-friendly chemical processes.^{4,5} Recently, nanometer-sized metallic particles have been developed as relevant catalysts for performing green organic transformation processes because of their outstanding intrinsic properties, combining the advantages of homogeneous and heterogeneous catalysts.^{6–9} Besides their pertinent activities owing to a high number of surface-exposed metal atoms and their original selectivities regarding to their unique surface structures and combined supramolecular assemblies,¹⁰ they could also provide improved recovery potentialities, which

constitute *sine qua non* conditions for eco-responsible applications.¹¹ Thus, the use of colloidal metallic particles finely dispersed in water constitutes one of the most effective and sustainable approaches to achieve the targeted recycling objective, through a biphasic water-substrate catalytic process.¹² For this purpose, highly water-soluble protective agents, such as surfactants,¹³ dendrimers¹⁴ or novel ligands such as N-heterocyclic carbenes^{15,16} are necessary to maintain the nano-species within the aqueous phase. More recently, as a class of nontoxic oligosaccharides, cyclodextrins have been extensively investigated in host-guest chemistry for construction of versatile supramolecular complexes owing to their special hydrophobic inner cavities.¹⁷ For instance, the inclusion complexation of randomly methylated cyclodextrins (RaMeCD) with an ammonium surfactant¹⁸ (HEA16Cl: *N,N*-dimethyl-*N*-hexadecyl-*N*-(2-hydroxyethyl)-ammonium chloride) or a sulfonated phosphine¹⁹ as guest molecules has been used to efficiently stabilize nano-sized ruthenium(0) hydrogenation catalysts in aqueous media and thus tune the catalytic performances of the metallic centers. Although ruthenium(0) nanospecies have been successfully protected by cyclodextrins alone,^{20,21} the less oxophilic rhodium metal proved to be more difficult to stabilize with the formation of visual aggregates. Based on these results, we investigated the use of original inclusion complexes formed between various cyclodextrins and ammonium surfactants as pertinent supramolecular assemblies to protect rhodium(0) species. These nanocatalysts were evaluated and compared in terms of stability, catalytic activity, and selectivity in the hydrogenation of various

^aEcole Nationale Supérieure de Chimie de Rennes, CNRS UMR 6226, 11 Allée de Beaulieu, CS 50837, 35708 Rennes Cedex 7, France. E-mail: alain.roucoux@ensc-rennes.fr; audrey.denicourt@ensc-rennes.fr; Fax: +33 02 2323 8199; Tel: +33 02 2323 8037

^bUniversité d'Artois, CNRS UMR 8181, Faculté des Sciences Jean Perrin, Rue Jean Souvraz, SP 18, F-62307 Lens Cedex, France

^cCNRS, LCC (Laboratoire de Chimie de Coordination), 205 Route de Narbonne, F-31077 Toulouse, France

^dUniversité de Toulouse, UPS, INPT, LCC, F-31077 Toulouse, France

† Electronic supplementary information (ESI) available: ITC thermograms and isotherms, T-ROESY NMR spectra of inclusion complexes and TEM pictures have been reported. See DOI: 10.1039/c6ra21851b

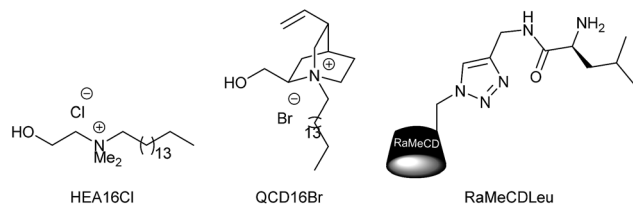


Fig. 1 Structure of CDs and surfactants.

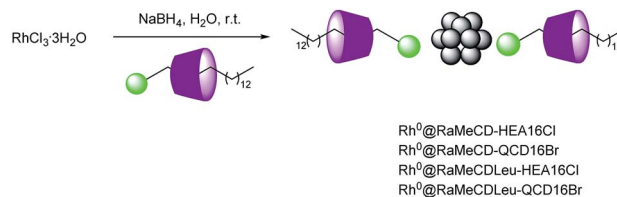
substrates: a functionalized olefin (methyl-2-acetamidoacrylate), an activated ketone (ethyl pyruvate) and acetophenone, a pertinent substrate in terms of chemoselectivity (aromatic ring *vs.* carbonyl group). Among the classical RaMeCD cyclodextrin or HEA16Cl ammonium salt, a methylated cyclodextrin grafted with a *L*-leucine moiety (RaMeCDLeu)²² and an optically active ammonium salt (QCD16Br = (1*S*,2*R*,4*S*,5*R*)-(+)-*N*-hexadecyl-5-vinyl-2-quinuclidinium-methanol bromide)²³ were also used as potential guest/host molecules to tune the selectivity, and potentially the asymmetric induction as a more challenging objective (Fig. 1).

Results and discussion

Design and characterization of rhodium(0) nanoparticles

The Isothermal Titration Calorimetry (ITC) measurements were achieved to check the stability and to determine equilibrium constants of the novel inclusion complexes obtained from the combination of methylated CDs with ammonium surfactants, including RaMeCD–QCD16Br, RaMeCDLeu–HEA16Cl and RaMeCDLeu–QCD16Br supramolecular assemblies (ESI-Fig. S1†). The association constant values (Table 1) were compared to the one of RaMeCD–HEA16Cl inclusion complex.

The association constants were found to be similar to that of RaMeCD–HEA16Cl inclusion complex. In fact, T-ROESY experiments indicated that the alkyl chain of ammonium surfactants was included inside the CD cavity whatever the inclusion complex (ESI-Fig. S2–S4†). According to the literature, dipolar contacts between the alkyl chain protons of the hexadecyltrimethylammonium bromide and protons inside the CD cavity provide a binding constant about $67\,700\text{ M}^{-1}$, as initially reported by Holzwarth²⁴ and more recently revised to $60\,733 \pm 11\,484\text{ M}^{-1}$ by B. Tutaj and coworkers.²⁵ Here, the slightly higher values achieved with the surfactants bearing a hydroxylated polar heads, could be attributed to the formation of a hydrogen bond between the flexible hydroxy



Scheme 1 Synthesis of rhodium(0) nanoparticles stabilized by methylated β -cyclodextrin/ammonium surfactant inclusion complexes.

groups of the surfactant's polar head and the CD.¹⁸ The thermodynamic parameters determined from ITC experiments also confirm that the surfactants have the same structural motif included into the β -CD cavity. Indeed, the inclusion processes are all mainly entropy driven, showing similar positive ΔS (Table 1). These results confirmed the formation of stable inclusion complexes between methylated CDs and hydroxylated ammonium surfactants, which could potentially be pertinent protective assemblies of rhodium(0) nanoparticles (Scheme 1).

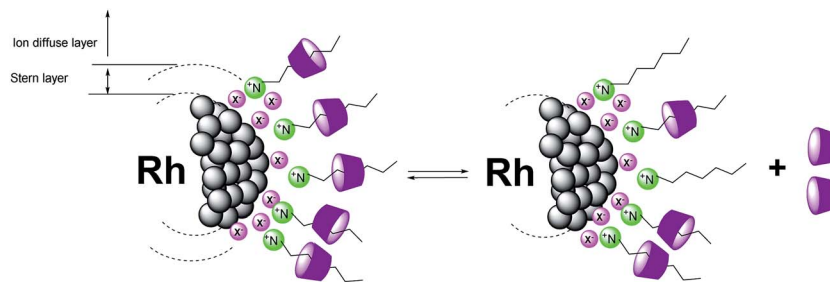
Rhodium(0) nanoparticles protected by these inclusion complexes were synthesized, using a two-step methodology as previously reported for the preparation of Ru⁰@RaMeCD–HEA16Cl NPs.¹⁸ The rhodium trichloride hydrate (RhCl₃·3H₂O) was chemically reduced, using sodium borohydride as reducing agent, in the presence of RaMeCD and HEA16Cl. As previously described in the literature^{18,26} the metallic surface is surrounded by a double layer of stabilizers (Scheme 2). The first layer is composed of surfactant molecules, whose polar head is directed towards the metallic surface, according to the adsorption of counter-ion to electron-deficient metal surfaces.^{27–29} The second layer is constituted of cyclodextrins interacting with the lipophilic tail of the surfactant.

The zeta potential value ζ of the well-dispersed Rh⁰@RaMeCD–HEA16Cl suspension, measured by electrophoretic light scattering (DLS spectroscopy), was used to determine the apparent charge of the nanoparticle in solution. A significant positive apparent charge of +50 mV for the rhodium species coated with RaMeCD–HEA16Cl assemblies was obtained as usually observed with ammonium stabilizers.³⁰ This value, which explains the good stability of the aqueous colloidal suspensions, characterizes the difference of potential between the solution far from the metal/solution interface (Stern layer based on adsorbed ionic species) and the mobile part of the disperse layer where salt concentration decreases when the distance increases.

Table 1 Thermodynamic data obtained by ITC of various inclusion complexes^a

Inclusion complex	$K\text{ (M}^{-1}\text{)}$	$\Delta G\text{ (cal mol}^{-1}\text{)}$	$\Delta H\text{ (cal mol}^{-1}\text{)}$	$-\Delta S\text{ (cal mol}^{-1}\text{)}$
RaMeCD–HEA16Cl	$84\,500 \pm 14\,700$	-6714 ± 104	856 ± 17	-7570 ± 121
RaMeCDLeu–HEA16Cl	$75\,200 \pm 12\,800$	-6645 ± 102	664 ± 18	-7309 ± 120
RaMeCD–QCD16Br	$96\,100 \pm 26\,800$	-6790 ± 170	237 ± 63	-7027 ± 233
RaMeCDLeu–QCD16Br	$91\,300 \pm 25\,400$	-6760 ± 169	212 ± 65	-6972 ± 234

^a Determined by isothermal titration calorimetry at 298 K.



Scheme 2 Proposed scheme for the supramolecular organization of inclusion complexes near the nanoparticle surface.

The RaMeCD/HEA16Cl ratio has been optimized since the use of a stoichiometric ratio leads to the destabilization of the rhodium(0) particles in the 1-tetradecene hydrogenation under standard conditions (1 bar H_2 , room temperature, 3 h). Two equivalents of each protective agents proved to be efficient for the stabilization of Rh^0 NPs, under atmospheric hydrogenation, as well as high pressure conditions (10 bar of H_2). The particle size, morphology and dispersion were determined by Transmission Electron Microscopy (TEM) analyses (ESI-Fig. S5–S7†).

Whatever the stabilizer association, the rhodium particles were well-dispersed on the grid, with spherical morphology. The Rh^0 NPs displayed a mean size in the range 1.2–1.5 nm, depending on the cyclodextrin/surfactant association. Based on the same surfactant (QCD16Br), the inclusion complex containing the more sterically hindered L-leucine-grafted cyclodextrin (Fig. 2a vs. Fig. 2c) led to the formation of larger NPs than the RaMeCD (1.5 nm vs. 1.2 nm, respectively). Similarly, compared to Rh^0 @RaMeCDLeu/QCD16Br system, the colloids stabilized by the RaMeCD combined with the less sterically hindered surfactant (HEA16Cl) exhibited slightly smaller diameters (1.3 nm vs. 1.5 nm) (Fig. 2b vs. Fig. 2c). In all cases, the metal core size of these original Rh^0 NPs were smaller than the host–guest inclusion complex-capped Ru^0 NPs with an average diameter of about 4 nm.¹⁸ This better control of the NPs growth could be easily explained by the presence of higher quantity of protective supramolecular assemblies (inclusion complex/Rh ratio = 2/1) which provide a better control during the growth step of the nanoparticles.

Catalytic hydrogenation using rhodium(0) nanoparticles

The catalytic performances of Rh^0 @RaMeCD–QCD16Br, Rh^0 @RaMeCDLeu–HEA16Cl and Rh^0 @RaMeCDLeu–QCD16Br NPs were evaluated in the hydrogenation of various model substrates, such as an activated olefin (methyl 2-acetamidoacrylate), an activated α -ketoester (ethylpyruvate) and an aromatic ketone (acetophenone).

The reduction of these prochiral compounds was carried out under pure biphasic conditions (water/substrate), at room temperature and under 10 bar of H_2 with 1 mol% of the nanocatalysts (cyclodextrins/surfactant/rhodium = 2/2/1) as optimized in 1-tetradecene hydrogenation (3 h, 10 bar of H_2 for 100% conv. vs. 20 h under 1 bar of H_2). These conditions were chosen in order to provide good yields in reduced products. Moreover, the stability of the triazole ring under the catalytic

reduction conditions was also checked. The conversion was monitored by gas chromatography analysis. The specific activity (SA) was calculated, considering an optimized reaction time for a complete conversion of the substrate and based on the total introduced amount of metal and not on the exposed surface metal. These specific activity values were clearly underestimated but were suitable from an economic point of view.

In a first set of experiments, RaMeCD–QCD16Br, RaMeCDLeu–HEA16Cl and RaMeCDLeu–QCD16Br rhodium nanocatalysts were evaluated in the reduction of methyl-2-acetamidoacrylate (Table 2).

Whatever the inclusion complexes (RaMeCD–QCD16Br, RaMeCDLeu–HEA16Cl or RaMeCDLeu–QCD16Br), the reduction of methyl 2-acetamidoacrylate occurred exclusively on the activated C=C double bond with complete conversion in an optimized 1.5 h time. It is noteworthy to report that the reduction of this substrate by Rh^0 suspensions, solely stabilized by cyclodextrins (RaMeCD or RaMeCDLeu), could not be achieved in these experimental conditions due to the destabilization of the nanocatalysts (Table 2, Entries 4 and 5). Finally, the use of the sole ammonium surfactant (HEA16Cl or QCD16Br) as protective agents leads to well stable colloidal suspensions with pertinent catalytic results in the reduction of methyl 2-acetamidoacrylate (Table 2, Entries 6 and 7). According to previous results based on similar investigations performed in our group,^{23,30} these efficient activities could be explained by the dynamic behaviour of the double layer which facilitates the access of the substrate at the particle's surface.

The reduction of the carbonyl function in ethylpyruvate as prochiral model substrate was also performed in similar reaction conditions (Table 3).

The transformation of ethylpyruvate into the corresponding alcohol was totally achieved, with various specific activities values according to the supramolecular assemblies in the following order: RaMeCDLeu–HEA16Cl > RaMeCDLeu–QCD16Br > RaMeCD–QCD16Br (SA of 67, 17 and 6 h^{-1} , respectively). These results could be justified by a more favorable displacement during the catalysis of free RaMeCDLeu vs. RaMeCD in the aqueous phase starting from inclusion complexes, as mentioned in Scheme 2, thus providing an efficient solubilisation of the organic substrate inside the RaMeCDLeu's cavity and a better diffusion towards the metal surface. Moreover, based on the observed conversions at 1.5 h (Table 3) and the comparison of the head group inside QCD16Br

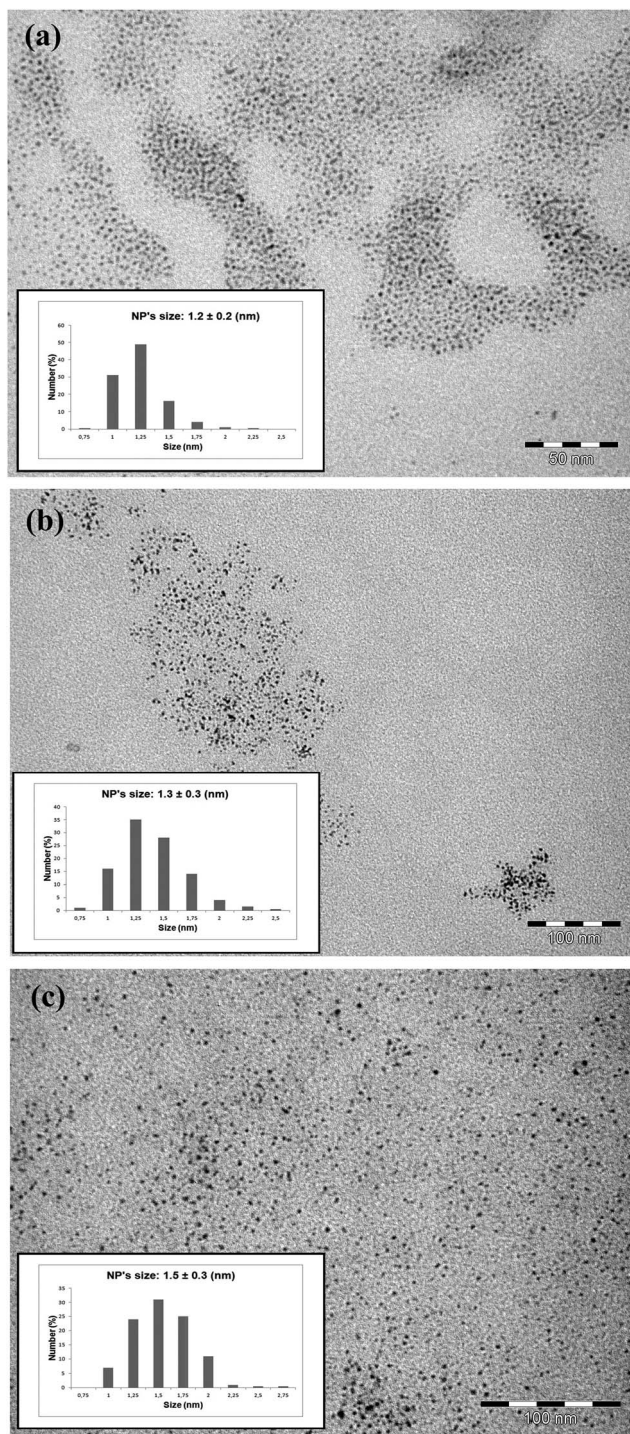
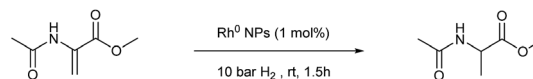


Fig. 2 TEM pictures and size distributions of (a) Rh^0 @RaMeCD-QCD16Br, (b) Rh^0 @RaMeCDLeu-HEA16Cl and (c) Rh^0 @RaMeCDLeu-QCD16Br NPs.

and HEA16Cl, it seems that kinetics is slower when the QCD16Br surfactant is located at the vicinity of the particle's surface, due to an increased steric hindrance, which probably limits the access of the substrate.

Finally, the chemoselectivity of the catalytic system was investigated towards the hydrogenation of acetophenone (reduction of the ketone *vs.* the aromatic ring (Table 4)).

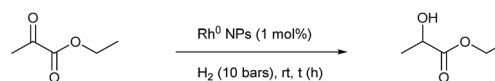
Table 2 Hydrogenation of methyl-2-acetamidoacrylate using rhodium(0) nanoparticles^a



Entry	Stabilizing agent	Conv. ^b (%)	SA ^c (h ⁻¹)
1	RaMeCD-QCD16Br	100	66.7
2	RaMeCDLeu-HEA16Cl	100	66.7
3	RaMeCDLeu-QCD16Br	100	66.7
4	RaMeCD ^d	n.d ^e	n.d ^e
5	RaMeCDLeu ^d	n.d ^e	n.d ^e
6	HEA16Cl	100 ^f	66.7
7	QCD16Br	100 ^f	66.7

^a Conditions: [substrate]/[Rh⁰] molar ratio = 100/1, 10 mL of aqueous suspension, 10 bar of H₂, rt, 1.5 h. ^b Determined by GC analysis. ^c Specific activity (SA) defined as number of mol of transformed substrate per mol of Rh per hour. ^d Formation of metal aggregates. ^e Non determined. ^f Not optimized time.

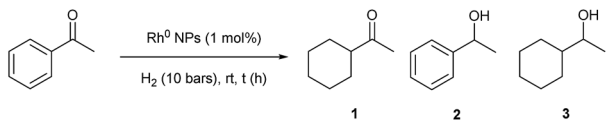
Table 3 Hydrogenation of ethylpyruvate using rhodium(0) nanoparticles^a



Entry	Stabilizing agent	Conv. at 1.5 h (%)	Time ^b (h)	SA ^c (h ⁻¹)
1	RaMeCD-QCD16Br	30	17 ^d	6
2	RaMeCDLeu-HEA16Cl	100	1.5	66.7
3	RaMeCDLeu-QCD16Br	45	6	17

^a Conditions: [substrate]/[Rh⁰] molar ratio = 100/1, 10 mL of aqueous suspension, 10 bar of H₂, rt. ^b Time for a complete conversion determined by GC analysis. ^c Specific activity (SA) defined as number of mol of transformed substrate per mol of Rh per hour. ^d Checked twice.

From kinetics investigations, two reaction pathways could be involved for the formation of the totally hydrogenated product (1-cyclohexylethanol 3), either *via* 1-cyclohexylethanone 1 from the reduction of aromatic ring, or either *via* 1-phenylethanol 2 from the reduction of carbonyl group. The higher ratio of 2 over 1 suggests that the carbonyl group is more easily reduced than the aromatic ring. However, the significant quantity of 1 (up to 24%) proves that the RaMeCD or RaMeCDLeu could not efficiently wrap the aromatic ring and avoid its hydrogenation. In addition, after 1.5 h of reaction, complete conversions were observed in the case of Rh⁰ NPs stabilized by the less sterically hindered inclusion complexes (RaMeCD-QCD16Br and RaMeCDLeu-HEA16Cl), compared to 60% conversion with Rh⁰@RaMeCDLeu-QCD16Br catalytic system. Increasing reaction time up to 3 h improved significantly the conversion by a factor of 2.5, however with a slightly destabilization of the Rh⁰ suspension with formation of aggregates. These results could be

Table 4 Hydrogenation of acetophenone using rhodium(0) nanoparticles^a


Entry	Stabilizing agent	Time (h)	1 : 2 : 3 ^b (%)
1	RaMeCD-QCD16Br	1.5	24 : 30 : 46
		3	12 : 0 : 88
2	RaMeCDLeu-HEA16Cl	1.5	13 : 48 : 39
		3 ^c	2 : 2 : 96
3	RaMeCDLeu-QCD16Br	1.5	16 : 28 : 16
		3 ^c	11 : 41 : 48

^a Conditions: [substrate]/[Rh⁰] molar ratio = 100/1, 10 mL of aqueous suspension, 10 bar of H₂, rt. ^b Selectivity determined by GC analysis. ^c Catalytic system started to be destabilized.

attributed to the competitive affinity of the substrate (acetophenone) and the surfactants inside the RaMeCDLeu's cavity. During the catalytic process, a partial release of the CDs in the bulk aqueous media allows the solubilisation of organic substrate by some free CDs (Scheme 2) and, as a consequence, enables a better diffusion of the substrates towards the metallic surface. Nevertheless, a strong affinity between organic substrate and CDs could disturb the dynamic organization of the protective agents around the NPs.

Unfortunately, no selectivities could be achieved with the use of chiral molecules as QCD16Br, RaMeCDLeu alone or associated, whatever the investigated prochiral substrate is (Tables 2–4). Based on previous investigations in our group on chiral ammonium-capped rhodium(0) nanocatalysts,²³ the lack of enantiodiscrimination during these asymmetric catalytic reactions could be attributed to a significant mobility of the inclusion complex at the metal surface in water. Moreover, in contrast with suitable coordinating ligands, the interaction of the HEA16Cl and QCD16Br surfactants within the particle's core seems to be too weak to provide asymmetric induction.

Conclusions

To conclude, the formation of supramolecular inclusion complexes between ammonium surfactant and cyclodextrin-based chiral molecules was investigated. The existence of a stable interaction between the surfactant and cyclodextrin was clearly evidenced by NMR spectroscopy and isothermal titration calorimetry measurements showed a strong affinity between the lipophilic chain of the surfactant and the hydrophobic cavity of cyclodextrin compounds, which was corroborated with their significant association constant values. These host-guest inclusion complexes were successfully used as pertinent supramolecular assemblies to protect rhodium(0) nanospecies. TEM analyses showed very small (1.2–1.5 nm) and well-dispersed spherical nanoparticles without aggregates.

According to optically active skeletons grafted on randomly methylated β -cyclodextrin (RaMeCDLeu) or surfactant (QCD16Br), these assemblies alone or associated produced a chiral environment onto the nanoparticle surfaces. Finally Rh⁰@RaMeCD-QCD16Br, Rh⁰@RaMeCDLeu-HEA16Cl and Rh⁰@RaMeCDLeu-QCD16Br were evaluated in the biphasic liquid-liquid hydrogenation of various functional groups (C=O, C=C) and demonstrated efficiencies in terms of stability and catalytic performances. During acetophenone hydrogenation, various differences in terms of conversions and selectivities relative to the competitive hydrogenation of the C=O bond *versus* the aromatic ring were observed, evidencing a direct impact of the steric hindrance of the supramolecular association. Nevertheless, in all cases, no significant induction was observed as expected. Finally, taking advantage of the supramolecular properties of assemblies to modulate the surface reactivity of nanoparticles, this original work may open new opportunities in the field of nanocatalysis and desirably in asymmetric reaction.

Experimental

Reagents and chemicals

N,N-Dimethyl-*N*-hexadecyl-*N*-(2-hydroxyethyl)ammonium chloride (HEA16Cl) and (1*S*,2*R*,4*S*,5*R*)-(+)-*N*-hexadecyl-5-vinyl-2-quinuclidinium-methanol bromide (QCD16Br) were synthesized from an already described procedure.^{23,30} Randomly methylated β -cyclodextrin (RaMeCD (1.8)) was purchased from Sigma-Aldrich. This cyclodextrin was partially methylated at positions 2, 3 or 6 and 1.8 hydroxyl groups per glucopyranose unit were statistically modified. *L*-Leucine-*N*-[(1-randomlymethylated- β -cyclodextrinyl-1*H*-1,2,3-triazol-4-yl) methylamide] (RaMeCDLeu) was prepared according to the procedure described in the literature.³¹

Rhodium(III) chloride hydrate was obtained from Strem Chemicals. Sodium borohydride and all substrates were purchased from Sigma-Aldrich, Acros Organics or Alfa Aesar and were used without further purification. Water was purified using Millipore Elix 5 (type MSP 100) system.

Analytical procedures

ITC analysis. Formation constants of methylated CD-ammonium surfactant complexes were determined by an isothermal calorimeter (ITC200, MicroCal Inc., USA), in a phosphate buffer (pH 6.5) at 298 K. In the case of RaMeCD, titrations of a 0.1 mM surfactant solution (QCD16Br or HEA16Cl) were realized with a 5 mM solution of RaMeCD. The inclusion ability of RaMeCDLeu was then investigated by competitive experiments with RaMeCD (injection of a 5 mM RaMeCD solution into a 0.1 mM surfactant–0.1 mM RaMeCDLeu solution). Each experiment was performed three times and consisted in the addition of an initial aliquot of 0.4 μ L, followed by ten injections of 3.7 μ L, delivered over 7.4 s, within a 204.5 μ L cell. Time interval between two consecutive injections was 60 s and agitation speed was 1000 rpm. The corresponding heat flow was recorded as a function of time, and the

heat effects due to dilution were taken into account by performing blank titrations. Binding constants were determined by nonlinear regression analysis of binding isotherms (obtained by integration of the raw signal) using a dedicated homemade program.³²

TEM analysis. Transmission electron microscopy (TEM) images were performed at the “Service Commun de Microscopie Electronique de l’Université Paul Sabatier” (UPS-TEMSCAN, Toulouse) and recorded with a JEOL 1011 electron microscope operating at 100 kV with resolution point of 4.5 Å. A drop of rhodium nanoparticles in water was deposited on a carbon-coated copper grid and dried in air. The size distributions were determined through a manual analysis of enlarged micrographs with Image J software using Microsoft Excel to generate histograms of the statistical size distribution and a mean diameter.

Dynamic light scattering spectroscopy. The zeta potential ζ of the nanoparticle aggregates were measured by dynamic light scattering (DLS) using a DelsaNano C instrument (Beckman Coulter). The aqueous suspensions of rhodium nanoparticles were analysed at 25 °C and measurements were started 10 min after the cell was placed in the DLS apparatus to allow the temperature to equilibrate.

Gas chromatography. For hydrogenation reactions, the conversion and the selectivity were determined by gas chromatography using Fisons Instruments GC 9000 series with FID detector equipped with a chiral Varian Chiralsil-Dex CB capillary column (30 m, 0.25 mm i.d.). Parameters were as follows: isotherm program with oven temperature, 90 °C (ethylpyruvate) or 130 °C (acetophenone and 2-acetamido acrylate); carrier gas pressure, 50 kPa.

General procedure for the preparation of surfactant/modified β -cyclodextrin stabilized rhodium(0) nanoparticles

$\text{RhCl}_3 \cdot 3\text{H}_2\text{O}$ (10 mg, 3.8×10^{-2} mmol, 1 eq.) was dissolved into distilled water (6 mL) and maintained under vigorous stirring. At the same time, cyclodextrin (RaMeCD or RaMeCDLeu) (7.6×10^{-2} mmol, 2 eq.) was added to a warm aqueous solution (14 mL) of appropriate surfactant (HEA16Cl or QCD16Br) (7.6×10^{-2} mmol, 2 eq.). The inclusion complex was stirred for 30 min before addition of sodium borohydride (3.6 mg, 9.5×10^{-2} mmol, 2.5 eq.). This mixture was quickly added to rhodium solution previously prepared above. The obtained rhodium nanoparticles were stirred for 24 h before used in catalytic test.

General procedure for atmospheric hydrogenation reactions

A 25 mL round bottom flask, charged with the aqueous colloidal rhodium(0) suspension (10 mL, 1.9×10^{-2} mmol) and appropriate substrate ([substrate]/ $[\text{Rh}^0]$ ratio = 100/1), was connected to a gas burette and a flask to balance the pressure. Then the system was filled with hydrogen ($P_{\text{H}_2} = 1$ bar) and the mixture was stirred vigorously at room temperature. Samples were collected from time to time to monitor the reaction by gas chromatography in previously mentioned conditions.

General procedure for high pressure hydrogenation reactions

The stainless steel autoclave was charged with the aqueous colloidal rhodium(0) suspension (10 mL, 1.9×10^{-2} mmol) and appropriate substrate ([substrate]/ $[\text{Rh}^0]$ ratio = 100/1). The autoclave was degassed three times and hydrogen gas was admitted to the system at a constant pressure (10 bar H_2). The mixture was stirred vigorously at room temperature. Samples were removed from time to time to monitor the reaction by gas chromatography in previously mentioned conditions.

Acknowledgements

The authors are grateful to CNRS and the Agence Nationale de la Recherche for the financial support of the SUPRANANO program (ANR-09-BLAN-0194). We also thank David Landy and Eléonore Bertaut (Université du Littoral Côte Opale) for Isothermal Titration Calorimetry measurements and Gregory Crowyn (Université d’Artois) for NMR measurements. We thank Buchler GmbH for Quinocridine precursor gift.

References

- 1 C. Descorme, P. Gallezot, C. Geantet and C. George, *ChemCatChem*, 2012, **4**, 1897–1906.
- 2 D. Prat, O. Pardigon, H.-W. Flemming, S. Letestu, V. Ducandas, P. Isnard, E. Guntrum, T. Senac, S. Ruisseau, P. Cruciani and P. Hosek, *Org. Process Res. Dev.*, 2013, **17**, 1517–1525.
- 3 R. A. Sheldon, *Green Chem.*, 2005, **7**, 267–278.
- 4 R. A. Sheldon, *Chem. Commun.*, 2008, 3352–3365.
- 5 J. M. Thomas, *Top. Catal.*, 2014, **57**, 1115–1123.
- 6 D. Astruc, in *Nanoparticles and Catalysis*, Wiley-VCH Verlag GmbH & Co. KGaA, Weinheim, 2008.
- 7 L. L. Chng, N. Erathodiyil and J. Y. Ying, *Acc. Chem. Res.*, 2013, **46**, 1825–1837.
- 8 V. Polshettiwar and R. S. Varma, *Green Chem.*, 2010, **12**, 743–754.
- 9 I. Geukens and D. E. de Vos, *Langmuir*, 2013, **29**, 3170–3178.
- 10 K. An and G. A. Somorjai, *ChemCatChem*, 2012, **4**, 1512–1524.
- 11 D. J. Cole-Hamilton and R. P. Tooze, in *Catalyst Separation, recovery and recycling: chemistry and process design*, Springer, 2006.
- 12 A. Denicourt-Nowicki and A. Roucoux, in *Nanomaterials in Catalysis*, ed. P. Serp and K. Philippot, Wiley-VCH Verlag & Co, Weinheim, 2013, pp. 55–95.
- 13 A. Denicourt-Nowicki and A. Roucoux, in *Metal Nanoparticles for Catalysis. Advances and Applications*, ed. F. F. Tao, Royal Society of Chemistry, Cambridge, 2014, pp. 99–111.
- 14 Y.-G. Ji and L. Wu, in *Dendrimers*, ed. H. B. T. Harris and L. Brian, Nova Science Publishers, Inc., Hauppauge, New York, 2013, pp. 249–263.
- 15 A. Ferry, K. Schaepe, P. Tegeder, C. Richter, K. M. Chepiga, B. J. Ravoo and F. Glorius, *ACS Catal.*, 2015, **5**, 5414–5420.
- 16 A. Rühling, H.-J. Galla and F. Glorius, *Chem.-Eur. J.*, 2015, **21**, 12291–12294.
- 17 G. Chen and M. Jiang, *Chem. Soc. Rev.*, 2011, **40**, 2254–2266.

- 18 C. Hubert, A. Denicourt-Nowicki, A. Roucoux, D. Landy, B. Léger, G. Crowyn and E. Monflier, *Chem. Commun.*, 2009, 1228–1230.
- 19 M. Guerrero, Y. Coppel, N. T. T. Chau, A. Roucoux, A. Denicourt-Nowicki, E. Monflier, H. Bricout, P. Lecante and K. Philippot, *ChemCatChem*, 2013, 5, 3802–3811.
- 20 A. Denicourt-Nowicki, A. Ponchel, E. Monflier and A. Roucoux, *Dalton Trans.*, 2007, 5714–5719.
- 21 N. T. T. Chau, S. Handjani, J. P. Guegan, M. Guerrero, E. Monflier, K. Philippot, A. Denicourt-Nowicki and A. Roucoux, *ChemCatChem*, 2013, 5, 1497–1503.
- 22 N. T. T. Chau, J. P. Guegan, S. Manuel, M. Guerrero, F. Hapiot, E. Monflier, K. Philippot, A. Denicourt-Nowicki and A. Roucoux, *Appl. Catal., A*, 2013, 467, 497–503.
- 23 E. Guyonnet Bilé, E. Cortelazzo-Polisini, A. Denicourt-Nowicki, R. Sassine, F. Launay and A. Roucoux, *ChemSusChem*, 2012, 5, 91–101.
- 24 H. Mwakibete, R. Cristantino, D. M. Bloor, E. Wyn-Jones and J. F. Holzwarth, *Langmuir*, 1995, 11, 57–60.
- 25 B. Tutaj, A. Kasprzyk and J. Czapkiewicz, *J. Inclusion Phenom. Macrocyclic Chem.*, 2003, 47, 133–136.
- 26 S. Gatard, L. Liang, L. Salmon, J. Ruiz, D. Astruc and S. Bouquillon, *Tetrahedron Lett.*, 2011, 52, 1842–1846.
- 27 S. Bucher, J. Hormes, H. Modrow, R. Brinkmann, N. Waldöfner, H. Bönemann, L. Beuermann, S. Krischok, W. Maus-Friedrichs and V. Kempter, *Surf. Sci.*, 2002, 497, 321–332.
- 28 J. D. Aiken, Y. Lin and R. G. Finke, *J. Mol. Catal. A: Chem.*, 1996, 114, 29–51.
- 29 A. Roucoux, J. Schulz and H. Patin, *Adv. Synth. Catal.*, 2003, 345, 222–229.
- 30 E. Guyonnet Bilé, R. Sassine, A. Denicourt-Nowicki, F. Launay and A. Roucoux, *Dalton Trans.*, 2011, 40, 6524–6531.
- 31 D. N. Tran, C. Blaszkiewicz, S. Manuel, A. Roucoux, K. Philippot, F. Hapiot and E. Monflier, *Carbohydr. Res.*, 2011, 346, 210–218.
- 32 E. Bertaut and D. Landy, *Beilstein J. Org. Chem.*, 2014, 10, 2630–2641.